



PERGAMON

INTERNATIONAL
JOURNAL OF
IMPACT
ENGINEERING

International Journal of Impact Engineering 26 (2001) 809–822

www.elsevier.com/locate/ijimpeng

HYPERVELOCITY PENETRATION MODELING: MOMENTUM VS. ENERGY AND ENERGY TRANSFER MECHANISMS

JAMES D. WALKER

Southwest Research Institute, San Antonio, Texas 78228-0510

Abstract—Analytic penetration modeling usually relies on either a momentum balance or an energy-rate balance to predict depth of penetration by a penetrator based on initial geometry and impact velocity. In recent years, fairly sophisticated models of penetration have arisen that develop the three-dimensional flow field within a target. Based on the flow field and constitutive assumptions, it is then possible to derive a momentum or an energy-rate balance. This paper examines the use of assumed flow fields within a target created by impact and then examines the resulting predicted behavior based on either momentum conservation or energy conservation. It is shown that for the energy-rate balance to work, the details of the energy transfer mechanisms must be included in the model. In particular, how the projectile energy is initially transferred into target kinetic energy and elastic compression energy must be included. As impact velocity increases, more and more energy during the penetration event is temporarily deposited within the target as elastic compression and target kinetic energy. This energy will be dissipated by the target at a later time, but at the time of penetration it is this transfer of energy that defines the forces acting on the projectile. Thus, for an energy rate balance approach to successfully model penetration, it must include the transfer of energy into kinetic energy within the target and the storage of energy by elastic compression. Understanding the role of energy dissipation in the target clarifies the various terms in analytic models and identifies their origin in terms of the fundamental physics. Understanding the modes of energy transfer also assists in understanding the hypervelocity result that penetration depth only slowly increases with increasing velocity even though the kinetic energy increases as the square of the velocity. © 2001 Elsevier Science Ltd. All rights reserved.

Keywords: Penetration mechanics, penetration modeling, energy transfer mechanisms, momentum conservation, energy conservation.

INTRODUCTION

Over the past few years, sophisticated models of penetration have been developed that rely on detailed models of how material within a target behaves during penetration. Given a model of target response, either an energy-rate balance or a momentum balance can be used to then obtain an equation of motion for the projectile. Integrated centerline momentum balances have produced good results, where the integral is taken along the centerline with an assumed velocity profile in the target and projectile (Walker and Anderson [1]). However, it is not possible to use a "global" energy balance in order for the energy-rate balance method to work. For an energy-rate balance model to work, it is necessary to take into account the mechanisms of energy transfer, and not just the global quantities.

An energy-rate balance model must include the intermediate stages detailing how energy is transferred to the target in kinetic and elastic compression forms, and not just deal with the fact that the energy is finally dissipated through plastic flow. In this regard, it is similar to the fact that for fluids the energy transfer mechanisms at the various scales in turbulent flow must be explicitly included in order to accurately model turbulence (known as the energy cascade, Hinze [2]). To give a penetration example, if the mechanism of the energy transfer process are ignored, and only the final plastic dissipation in the target is included, consider for simplicity a case of rigid penetration. If the projectile penetrates a metal target with a given plastic dissipation per unit depth dW/dh , based on the flow within the target, and only the final dissipation leads to energy loss by the projectile, then the final depth of penetration would be given by

$$\text{depth} \sim \frac{(E_k)_0}{dW/dh} = \frac{\text{initial kinetic energy}}{\text{dissipation per unit depth}} \quad (1)$$

This assumption predicts that penetration behaves as the velocity squared. Though true for non-deforming projectiles at low velocities, it is not true for high velocities. When one carefully goes through the energy-rate balance and compares it to a momentum balance, the term that is missing is a $(1/2)\rho v^2$ term. In order for this term to be in an energy rate balance, it is necessary to include the intermediate energy transfer into kinetic energy and elastic compressive energy in the target.

This paper explores how energy is initially transferred to the target through four examples. First, energy partitioning in 1-D planar impact will be examined. It will be shown that the energy is evenly divided between kinetic and internal energy, and that most of the internal energy initially goes into elastic compression. Second, a problem of pure shear will be examined where elastic energy is minimal due to the absence of compressions and temporary storage of kinetic energy in the target for later dissipation does not occur. It is shown for this case that a momentum-based model and an energy-rate based model produce the same result, independent of speed. Next, a 2-D cylindrical cavity expansion is considered, to examine how the energy is partitioned there between kinetic, compressive, and plastically dissipated energy. Again it will be shown that roughly half the energy initially goes into kinetic energy and half goes into internal energy, again with most going into elastic compression. Finally, the case of eroding penetration will be examined. It will be shown that the initial transfer of energy to the target in the form of kinetic and elastic energy is correlated with the $(1/2)\rho v^2$ resistive force that arises in the momentum balance. Finally, detailed hydrocode calculations examine the energy partitioning in the target between elastic, dissipated, and kinetic energies for a range of velocities. These results show that the mechanics of the energy transfer must be included in any model based on an energy-rate balance. Any energy-rate balance based model that does not include these effects cannot work for higher velocities.

THE PLASTIC DISSIPATION RATE

To do an energy-rate balance for penetration problems, a necessary mechanism to understand is plastic dissipation within the target. Plastic flow dissipates energy and is irreversible. A basic assumption of plasticity theory is that deformation can be partitioned into elastic and plastic parts: i.e., that the rate of deformation tensor $D_{ij} = (\partial v_i / \partial x_j + \partial v_j / \partial x_i) / 2$ can be written

$$D_{ij} = D_{ij}^e + D_{ij}^p \quad (2)$$

(see Hill [3], Lubliner [4], Malvern [5]). Stress arises from the elastic deformation through Hooke's law. A yield criterion is a requirement placed on the stress: the von Mises yield criterion says that the second invariant of the stress deviator tensor cannot exceed a constant based on the flow stress $((1/2)s_{ij}s_{ij} \leq Y^2/3)$, and the Tresca yield criterion says that the maximum shear stress cannot exceed the flow stress (e.g. $|\sigma_{\theta\theta} - \sigma_{rr}| \leq Y$). When strict equality holds the material is plastically flowing—part of the deformation is plastic. Plastic flow is called associated when the direction of the plastic flow is obtained by differentiating the yield criterion with respect to the stress. In this paper plastic flow will be associated.

The plastic dissipation rate is defined as the work done by the plastic deformation:

$$\dot{W}_p \equiv \sigma_{ij} D_{ij}^p \quad (3)$$

Plastic flow is assumed incompressible ($D_{ii}^p = 0$). For the von Mises yield criterion the plastic dissipation can be written:

$$\dot{W}_p = Y \dot{\epsilon}^p \quad \text{where} \quad \dot{\epsilon}^p \equiv \sqrt{\frac{2}{3} D_{ij}^p D_{ij}^p} \quad (4)$$

The square root term is referred to as the equivalent plastic strain rate. In this paper it is assumed the velocity is continuous and that there is no need to consider internal slip (which can be addressed through shearing surfaces). The plastic dissipation rate is

$$\dot{W}_p = \int_{\Omega} \dot{W}_p d\Omega = \int_{\Omega} Y \dot{\epsilon}^p d\Omega \quad (5)$$

This rate will be used in examining how energy is deposited in the target for four specific examples.

The energy stored elastically is computed in a similar fashion. With the stress given by $\sigma_{ij} = \lambda \epsilon_{kk} \delta_{ij} + 2G \epsilon_{ij}^e$, where ϵ_{ij}^e is the strain, the Lamé constant $\lambda = K - (2/3)G$, K is the bulk modulus and G is the shear modulus, the elastic energy is

$$e_e \equiv \int \sigma_{ij} d\epsilon_{ij}^e = \frac{1}{2} \lambda (\epsilon_{kk}^e)^2 + G \epsilon_{ij}^e \epsilon_{ij}^e = \frac{1}{2} \frac{p^2}{K} + \frac{s_{ij} s_{ij}}{4G} \quad (6)$$

and the total elastic energy is

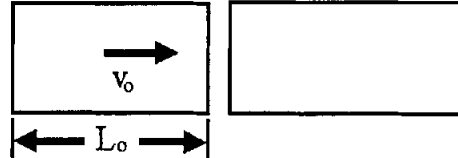
$$E_e = \int_{\Omega} e_e d\Omega \quad (7)$$

ENERGY PARTITIONING IN ONE-DIMENSIONAL IMPACT

An impactor of thickness L impacts a semi-infinite target of like material (Fig. 1). The impact produces a wave running in both directions from the impact surface with particle velocity one half the impact velocity. If the target and projectile material is a fluid with an equation of state

$$p = K(\rho/\rho_0 - 1) \quad (8)$$

where K is the bulk modulus and ρ_0 is the initial density, then an energy balance for when the shock front traveling at velocity c reaches the back of the projectile is



$$\frac{1}{2} \rho_0 L_0 v_0^2 = 2 \frac{1}{2} \rho L \left(\frac{1}{2} v_0 \right)^2 + 2L \frac{1}{2} K \left(\frac{\rho}{\rho_0} - 1 \right)^2 \quad (9) \quad \text{Fig. 1. One-dimensional impact geometry.}$$

The left hand side of the equation is the initial kinetic energy, and the right hand side has the first term of kinetic energy and the second of energy stored in elastic compression (these latter terms have a factor of 2 since they represent both the target and projectile). Mass conservation gives that $\rho_0 L_0 = \rho L$ which gives

$$\frac{1}{2} \rho_0 L_0 v_0^2 = \frac{1}{4} \rho_0 L_0 v_0^2 + L K \left(\frac{\rho}{\rho_0} - 1 \right)^2 \quad (10)$$

The first conclusion is that for a symmetric impact, the energy partitioning between elastic and kinetic energy is independent of velocity: half the initial kinetic energy goes into kinetic energy in the projectile and target, and half the initial kinetic energy goes into elastic compression in the projectile and target.

Given an equation of state, it is possible to explicitly calculate the shock front speed using the energy balance combined with the mass balance. The length of the compressed region is

$$L = ct - (1/2)v_0 t \quad \text{where} \quad L_0 = ct \quad (11)$$

Mass conservation thus gives $\rho/\rho_0 = c/(c - v_0/2)$ and, inserting in Eq. (10), the shock front speed is then

$$c = v_0/4 + \sqrt{K/\rho_0 + v_0^2/16} \quad (12)$$

This result is precisely that obtained through use of the mass and momentum Hugoniot jump conditions ($P = \rho_0 c u_p$). (The fact that they agree is a special case because of the linearity of the equation of state—for this deformation, slow uniaxial loading coincides with the Rayleigh line. In general, shocks dissipate additional energy.) Thus, in order for the energy equation to give the same result as the momentum equation, it is necessary to include the elastic compression energy.

What happens to the energy partitioning when an elastic-plastic solid is introduced? First, the partitioning of the initial kinetic energy of half into kinetic energy and half into internal energy is maintained. Now some of the internal energy goes into dissipated plastic work and some goes into elastic recoverable energy. For one-dimensional uniaxial strain loading for a perfectly elastic-plastic solid with a flow stress of Y , the incremental loading conditions in the plastically flowing region give rise to the following partition between elastic and plastic deformation:

$$D_{xx}^e = \frac{1}{3} D_{xx}, \quad D_{xx}^p = \frac{2}{3} D_{xx}, \quad D_{yy}^e = D_{zz}^e = \frac{1}{3} D_{xx}, \quad D_{yy}^p = D_{zz}^p = -\frac{1}{3} D_{xx} \quad (13)$$

The equivalent plastic strain rate is $\dot{\epsilon}^p = (2/3) |D_{xx}|$, and so for a given strain ϵ_{xx} the compression work that went into elastic and into plastic parts is given by

$$e_e = \frac{1}{2} K \epsilon_{xx}^2 + \frac{Y^2}{6G}, \quad w_p = \frac{2Y}{3} \left(|\epsilon_{xx}| - \frac{Y}{2G} \right) \quad (14)$$

(In the above, $\epsilon_{HEL} = Y/2G$ is the yielding strain and $Y^2/6G$ is the elastic energy stored in the stress deviators when the material is flowing.) Using this, it is possible to plot the partition between elastic internal energy and dissipated energy, in particular for the specific case of steel with $\rho_0 = 7.85 \text{ g/cm}^3$, $K = 1.67 \text{ MBar}$, $G = 0.77 \text{ MBar}$ and $Y = 1.2 \text{ GPa}$ (Fig. 2). Initially there is no plastic strain until the HEL strain is reached, and then the ratio of plastic work to total work (energy) rises to a little over 20% before rapidly dropping off as velocity increases. Thus, only for low velocities is the energy going immediately into dissipation appreciable; and even then, most energy goes into kinetic and elastic forms.

Though penetration is a 2-D/3-D process, the result of the 1-D analysis shows that the initial energy transfer from the penetrator to the target is predominantly in the form of kinetic energy in the target and elastic compression energy of the target. At later time, these elastic compressions will release, and the energy will be distributed in a different fashion. However, during the "penetration," the force the impactor sees is related to the energy being transferred at that time. Thus the behavior of the projectile is determined by the partitioning of energy within the target.

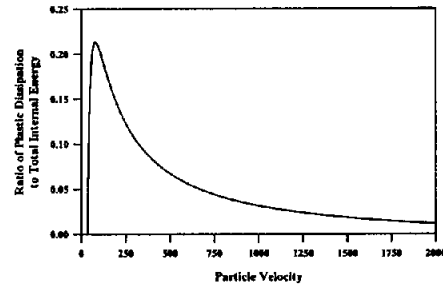


Fig. 2. Internal energy partition for uniaxial strain/one-dimensional impact.

PURE SHEAR

The problem of pure shear demonstrates that, when elastic compressions and kinetic energy transfer in the target are not important, the momentum approach to solving the problem and the global energy-rate balance approach give the same answer (Walker [6]). Once again, for simplicity of analysis it will be assumed that the projectile and target are made of the same material. A "projectile" of thickness R is connected to an infinite half space of "target" material (Fig. 3). There is an initial velocity distribution within the target material, which will be denoted $v_0(y)$, and the projectile has initial velocity $v_0(0) = V$. The flow stress of the elastic-plastic material is Y . There is no slip between the projectile and the elastic-plastic material.

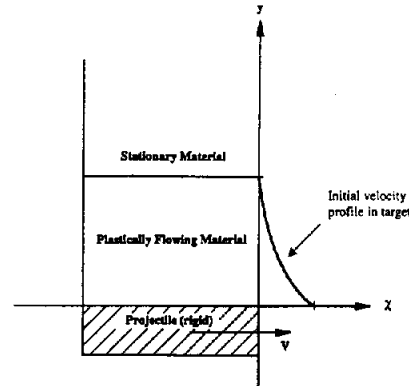


Fig. 3. Shear geometry.

First an elastic-plastic solution to the problem will be presented. When the pure shear problem is run on a hydrocode, it is seen that an elastic shear wave is formed which travels from the free surface of the projectile to the initial assumed velocity gradient in the target and reflects there, reducing the velocity, and the shear wave travels back again to the projectile free surface, and the process is repeated. The elastic-plastic shear problem is thus a wave propagation problem. With each passage of the wave, the material velocity is reduced. This continues until the target material response is entirely elastic, at which point the projectile has nearly come to rest. The assumption that the projectile and target have the same density and shear modulus precludes reflections at the target/projectile interface.

Elastic deformation in both the target and projectile can be written as a displacement $u_x = g(y, t)$. The shear strain is $\epsilon_{xy} = (1/2)\partial g/\partial y$, and the resulting shear stress is $\sigma_{xy} = 2G\epsilon_{xy} = G\partial g/\partial y$. Placing these terms in the momentum balance gives the wave equation $\partial^2 g/\partial t^2 = c_s^2 \partial^2 g/\partial y^2$ where $c_s = \sqrt{G/\rho}$ is the shear wave speed. An elastic wave travelling from the plastic region to the free surface of the projectile can be represented as $g = g(y + c_s t)$. From this, the particle velocity (the actual speed of the material behind the wave front) can be determined: particle velocity $= \partial g/\partial t = c_s g'$. The stress wave will have the maximum elastic stress allowed. For pure shear, the maximum stress from the von Mises yield criterion is $-Y/\sqrt{3}$. Thus,

$$-\frac{Y}{\sqrt{3}} = 2G\epsilon_{xy} = Gg' \quad (15)$$

The elastic wave has a particle velocity of

$$\text{particle velocity} = c_s g' = 2c_s \epsilon_{xy} = -c_s \frac{Y/\sqrt{3}}{G} \quad (16)$$

When the elastic shear wave reflects from the free surface of the projectile, it returns in the form $-g(y - c_s t)$, since the surface is traction free. The change in particle velocity at the surface of the projectile is then

$$\Delta v = -c_s \frac{Y/\sqrt{3}}{G} - c_s \frac{Y/\sqrt{3}}{G} = -2c_s \frac{Y/\sqrt{3}}{G} \quad (17)$$

or the change in particle velocity at the free surface is twice the particle velocity of the wave—a well known result.

The plastically shearing material reflects like a free surface because of the nonlinear material response. The elastic wave cannot be superimposed on the plastic response, and for the shear problem a total reflection of the elastic wave occurs when the elastic wave returning from the free surface of the projectile arrives at the elastic-plastic interface. To calculate the deceleration, the change in velocity is divided by the travel time of the wave. As the problem progresses the distance of the return trip is greater, due to the initial velocity profile in the target. If Δt is the time of the round trip of the wave, then

$$\Delta t = \frac{v_0^{-1}(V) + R + R + v_0^{-1}(V + \Delta v)}{c_s} \quad (18)$$

where V is the velocity of the projectile and v_0^{-1} is the inverse of the initial velocity profile in the target. An approximate equation of motion for the projectile is

$$\frac{dV}{dt} \approx \frac{\Delta v}{\Delta t} = -\frac{2Y/\sqrt{3}\rho}{2R + v_0^{-1}(V) + v_0^{-1}(V + \Delta v)} = -\frac{Y/\sqrt{3}\rho}{R + v_0^{-1}(V) - c_s(Y/\sqrt{3}G)(v_0^{-1})'(V)} \quad (19)$$

Now an energy-rate balance solution to the problem will be derived. Noting how the velocity decreases due to the elastic waves, the assumed form of the solution will be (Fig. 4)

$$v_x = \begin{cases} v_0(\tilde{y}), & -R \leq y < \tilde{y} \\ v_0(y), & \alpha R \leq y \end{cases} \quad (20)$$

where $v_y = v_z = 0$, $v_0(y)$ is the initial velocity distribution in the target, assumed to be differentiable and strictly decreasing, and $\tilde{y}(t)$ is a time dependent variable describing the location of the elastic-plastic interface. All the material to the left of the interface ($y \leq \tilde{y}(t)$) behaves as a rigid body, while material to the right (with $v_0(y) > 0$) is plastically shearing. With the assumed velocity field, the kinetic energy can be calculated:

$$\begin{aligned} E_K &= \int_{-R}^{\infty} \frac{1}{2} \rho v^2 dy \\ &= \frac{1}{2} \rho R V^2 + \frac{1}{2} \rho \tilde{y} V^2 + \int_{\tilde{y}}^{\infty} \frac{1}{2} \rho v_0^2(y) dy \end{aligned} \quad (21)$$

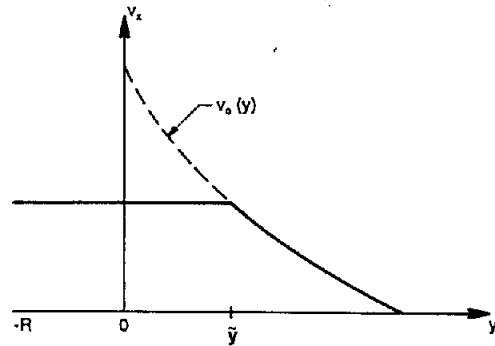


Fig. 4. Energy-rate balance velocity profile.

where $V = v_0(\tilde{y})$ is the projectile velocity (which equals the velocity of the target material to the left of \tilde{y}). Differentiation with respect to time gives

$$\dot{E}_K = \rho(R + \tilde{y})V\dot{V} \quad (22)$$

For the pure shear geometry considered here, all the deformation is assumed plastic and the local dissipation is

$$\dot{w}_p = Y \sqrt{\frac{1}{3} \left(\frac{\partial v_x}{\partial y} \right)^2} = \frac{Y}{\sqrt{3}} \left| \frac{\partial v_x}{\partial y} \right| \quad (23)$$

and the total dissipation is

$$W_p = \int_0^{\alpha R} \dot{w}_p dy = \frac{YV}{\sqrt{3}} \quad (24)$$

With the kinetic energy and the rate of dissipation, the energy rate balance is

$$\dot{E}_K + \dot{W}_p = 0 \quad \Rightarrow \quad \rho(R + v_0^{-1}(V))\dot{V} = -\frac{Y}{\sqrt{3}} \quad (25)$$

This equation is qualitatively similar to that derived by the elastic-plastic approach (Eq. (19)), and in the limit as $G \rightarrow +\infty$ the two equations are identical. As an example of an explicit solution, if the initial velocity in the target is linear and is expressed by $v_0(y) = V_0(1 - y/R)$, then $v_0^{-1}(V) = R(1 - V/V_0)$ and Eq. (25) can be integrated using $\dot{V} = VdV/dx$ to calculate the final distance of travel X before the projectile comes to rest:

$$X = \frac{(2/3)RV_0^2}{Y/\sqrt{3}} \quad (26)$$

The distance of travel is the initial kinetic energy in the system (target plus projectile) divided by the dissipation per unit distance, as predicted by the naive global argument presented in the introduction.

The shear problem thus behaves in a simple manner at any speed. Issues of transferring kinetic energy to the target that is later dissipated elsewhere or of target compressibility do not arise. That the momentum balance and the energy-rate balance agree for the case of pure shear shows that the notion of examining the plastic dissipation is qualitatively correct, but that the specific mechanisms of energy transfer arising in penetration of targets by projectiles must be taken into account.

TWO-DIMENSIONAL CYLINDRICAL CAVITY EXPANSION

To determine how the energy is transferred during the penetration event, it is most relevant to examine a two-dimensional cylindrical cavity expansion (Fig. 5) (Crozier and Hunter [7], Forrestal, *et al.* [8], Forrestal and Luk [9], Walker and Anderson [1]). The presentation here begins with results in Walker and Anderson. A linear pressure dependence and elastic-perfectly plastic behavior with a Tresca yield criterion ($\sigma_{\theta\theta} - \sigma_{rr} = Y$) are assumed along with a similarity transformation $\xi = r/ct$ to reduce the mass and momentum balance equations to

$$v' + \frac{v}{\xi} = \frac{1}{K}(-c\xi + v)\sigma'_r, \quad \sigma'_r - \frac{Y}{\xi} = \rho(-c\xi + v)v' \quad (27)$$

In this expression σ_r is the radial stress and c is the speed of the elastic-plastic interface. Assuming that $Y/K \ll 1$ and that $-c\xi + v \approx -c\xi$ leads to:

$$v(\xi) = -\frac{Y}{\rho c \xi} + c_3 \frac{\sqrt{K/\rho c^2 - \xi^2}}{\xi} \quad \text{where} \quad c_3 = \frac{Y/\rho + V^2}{\sqrt{K/\rho - V^2}} \quad (28)$$

The relationship between the elastic-plastic interface velocity and the cavity expansion velocity is

$$\left(1 + \frac{\rho V^2}{Y}\right) \sqrt{K - \rho c^2} = \left(1 + \frac{\rho c^2}{2G}\right) \sqrt{K - \rho V^2} \quad (29)$$

Defining the bulk sound speed as $c_0 \equiv \sqrt{K/\rho}$, it can be shown that for cavity expansion velocities $V \geq 0.2c_0$ the elastic-plastic interface velocity is nearly the bulk sound speed, i.e. $c \approx c_0$. For a fluid with no shear strength, $c = c_0$ exactly. Since the interest here is in high velocity penetration, it will be assumed that the shear strength is negligible when computing the kinetic energy and elastically stored energy. This assumption greatly simplifies the expressions and allows us to ignore the elastic precursor. With this assumption, the velocity becomes

$$v(\xi) = c_3 \frac{\sqrt{1 - \xi^2}}{\xi} \quad \text{where} \quad c_3 = \frac{V\xi}{\sqrt{1 - \xi^2}}$$

$$\text{and } \xi \equiv V/c \equiv 1/\alpha$$

(30)

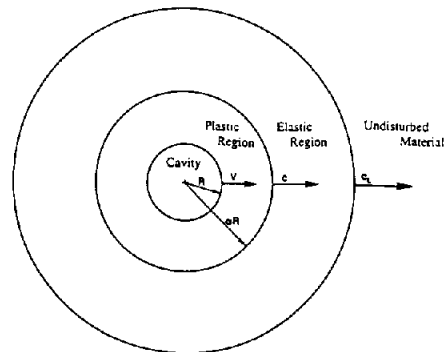


Fig. 5. Cylindrical cavity expansion geometry.

Placing this expression back into Eq. (27) gives the stress as

$$\sigma_r(\xi) = -\rho c c_3 \ln \left(\frac{\sqrt{1-\xi^2}}{\xi} + \frac{1}{\xi} \right) \quad (31)$$

where it has been assumed that $\sigma_r(1) = 0$.

The square of the velocity can be integrated to give the kinetic energy at time $t = R/V$:

$$E_k = \int_{V_i}^{\alpha} \frac{1}{2} \rho v^2 2\pi r dr = 2\pi (ct)^2 \int_{\xi}^1 \frac{1}{2} \rho v^2(\xi) \xi d\xi = \frac{1}{2} \rho V^2 \pi R^2 \left(\frac{-2 \ln(\xi)}{1-\xi^2} - 1 \right) \quad (32)$$

Similarly, an estimate of the energy stored in elastic compression is given by

$$E_e \approx \int_{V_i}^{\alpha} \frac{\sigma_r^2}{2K} 2\pi r dr = \frac{1}{2} \rho V^2 \pi R^2 \left[\frac{-\xi^2}{1-\xi^2} \ln^2 \left(\frac{\sqrt{1-\xi^2}}{\xi} + \frac{1}{\xi} \right) + \frac{2}{\sqrt{1-\xi^2}} \ln \left(\frac{\sqrt{1-\xi^2}}{\xi} + \frac{1}{\xi} \right) + 2 \frac{\ln(\xi)}{1-\xi^2} \right] \quad (33)$$

To estimate the amount of energy dissipated due to plastic deformation, it is necessary to determine the partitioning between elastic and plastic deformation, similar to what was done for one-dimensional uniaxial strain. In this case, the Tresca yield criterion is being used with $\sigma_{\theta\theta} - \sigma_{rr} = Y$. It is possible to show that $\sigma_{rr} > \sigma_{zz} > \sigma_{\theta\theta}$ and therefore there is no plastic straining in the z -direction and $D_{rr}^p = -D_{\theta\theta}^p$ since the flow is associated. The rate of deformation decomposes into

$$D_{rr}^e = D_{\theta\theta}^e = (D_{rr} + D_{\theta\theta})/2, \quad D_{rr}^p = -D_{\theta\theta}^p = (D_{rr} - D_{\theta\theta})/2, \quad D_{zz}^e = D_{zz}^p = 0 \quad (34)$$

With this, the plastic work is

$$\dot{W}_p = \int \sigma_{ij} D_{ij}^p d\Omega = \int (\sigma_{rr} - \sigma_{\theta\theta}) D_{rr}^p d\Omega = - \int Y D_{rr}^p d\Omega = - \int Y \frac{1}{2} (D_{rr} - D_{\theta\theta}) d\Omega \quad (35)$$

The velocity (Eq. (30)) gives the following rate of deformation

$$D_{rr} = \frac{\partial v}{\partial r} = -\frac{c_3}{ct \xi^2 \sqrt{1-\xi^2}}, \quad D_{\theta\theta} = \frac{v}{r} = \frac{c_3 \sqrt{1-\xi^2}}{ct \xi^2}, \quad D_{zz} = \frac{\partial v_z}{\partial z} = 0 \quad (36)$$

The total plastic dissipation rate is then

$$\dot{W}_p = - \int_{V_i}^{\alpha} Y \frac{1}{2} (D_{rr} - D_{\theta\theta}) 2\pi r dr = 2\pi R V Y \left\{ \frac{2}{\sqrt{1-\xi^2}} \ln \left(\frac{\sqrt{1-\xi^2}}{\xi} + \frac{1}{\xi} \right) - 1 \right\} \quad (37)$$

To obtain the total plastic work, this expression is integrated from the cavity at zero radius to radius Vt using $\int R V dt = (1/2) R^2$. The result is

$$W_p = \pi R^2 Y \left\{ \frac{2}{\sqrt{1-\xi^2}} \ln \left(\frac{\sqrt{1-\xi^2}}{\xi} + \frac{1}{\xi} \right) - 1 \right\} \quad (38)$$

These results allow a determination of how the energy is being partitioned as the cavity is expanded. For the steel with material properties stated above, Fig. 6 shows the relative amounts of the total energy deposited in the material as a function of cavity expansion velocity (the plot covers values of ξ from 0.1 to 0.9). For example, the relative amount of kinetic energy is given by $E_k/(E_k + E_e + W_p)$. The results are similar to those seen in the 1-D impact: nearly half the energy goes into kinetic energy and half is divided between elastic compression and dissipated plastic flow, with most of the latter half going into elastic compression. Thus, even though once the forced cavity expansion stops most of the energy will be dissipated through plastic flow as the expansion is brought to rest, the energy transfer mechanism is first

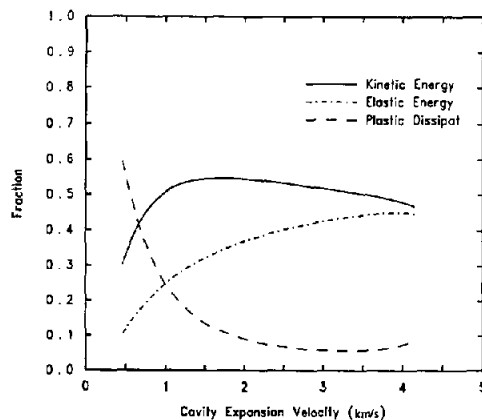


Fig. 6. Energy partition in cylindrical cavity expansion.

into kinetic and elastic energy. The force required to open the cavity depends on the how the energy transfer is partitioned.

PENETRATION

Finally, the penetration of a projectile into a metal target is considered. For eroding flow, hydrocode calculations show that the target flow is hemispherical. With assumed velocities in the target and projectile, the centerline momentum balance solution to this problem is (Walker and Anderson [1])

$$\rho_p \dot{v}(L-s) + u \left\{ \rho_p s + \rho_p R \frac{\alpha-1}{\alpha+1} \right\} + \rho_p \left(\frac{v-u}{s} \right) \frac{s^2}{2} + \rho_p \dot{\alpha} \frac{2Ru}{(\alpha+1)^2} = \frac{1}{2} \rho_p (v-u)^2 - \left\{ \frac{1}{2} \rho_p u^2 + \frac{7}{3} \ln(\alpha) Y_t \right\}$$

$$\dot{v} = -\frac{\sigma_p}{\rho_p(L-s)} \left\{ 1 + \frac{v-u}{c} + \frac{s}{c} \right\}, \quad \dot{L} = -(v-u) \quad (39)$$

where R is the radius of the crater, L is the length of the projectile, ρ_t is the density of the target, ρ_p is the density of the projectile, v is the projectile back end velocity, u is the target-projectile interface velocity (penetration velocity), c is the wave speed in the projectile, Y_t is the target yield strength, σ_p is the projectile yield strength, s is the extent of the plastic zone within the projectile and α is the extent of the plastic zone in the target in crater diameters. The cavity expansion technique (Eq. (29)) provides α , and matching velocity slopes determines s . The first equation above is the centerline momentum balance, the second is the deceleration of the projectile through reflecting elastic waves, and the final equation is the erosion of the projectile.

The centerline momentum balance is arrived at through assumed velocity profiles within the target and projectile. The velocity field within the target is of primary interest, and will be presented in detail. The target velocity field also is used to calculate the $(7/3) \ln(\alpha) Y_t$, which arises through assumptions about the shear stress within the target and its derivative along the axis of symmetry.

The model in Eqs. (39) has been shown to give good results over many impact conditions. To compare this model, based on a momentum balance, directly with an energy-rate balance, it will be necessary to examine the velocity field within the target in detail. This velocity field is based on the observation from large scale numerical simulations that the velocities within the target have a hemispherical quality to them. To write such a velocity field, it is natural to work in spherical coordinates. The cylindrical symmetry of the problem implies no ϕ dependence and $v_\phi = 0$. There is no radial component to the velocity at the top of the flow field (where $\theta = \pi/2$), and the flow is purely radial when $\theta = 0$. A vector potential yielding such a velocity field is

$$\vec{A} = f(r) \sin(\theta) \hat{e}_\phi \quad (40)$$

The curl is taken in spherical coordinates (Malvern [5]) assuming no ϕ dependence:

$$\vec{v}(r, \theta) = \text{curl}(\vec{A}) = \frac{1}{r \sin(\theta)} \frac{\partial}{\partial \theta} (A_\phi \sin(\theta)) \hat{e}_r - \frac{1}{r} \frac{\partial}{\partial r} (r A_\phi) \hat{e}_\theta + \left[\frac{1}{r} \frac{\partial}{\partial r} (r A_\theta) - \frac{1}{r} \frac{\partial A_r}{\partial \theta} \right] \hat{e}_\phi \quad (41)$$

yielding

$$v_r(r, \theta) = \frac{2f}{r} \cos(\theta), \quad v_\theta(r, \theta) = -\frac{1}{r} \frac{d(rf)}{dr} \sin(\theta) \quad (42)$$

This formulation has the advantage of there being only one unknown function f .

Along the axis of symmetry, the velocity is $v_r(r, 0) = 2f/r$. Thus, the velocity along the centerline determines $f(r)$ and so completely determines \vec{v} . A convenient choice for f is

$$f(r) = ar + \frac{b}{r} + c \quad (43)$$

where a , b , and c are constants. This gives rise to terms of the form a , b/r^2 , and c/r in the velocity. The b/r term drops out of v_θ , which can greatly simplify algebraic expressions. In particular, if c is arbitrarily set to zero,

$$v_r(r, \theta) = \left(2a + \frac{2b}{r^2} \right) \cos(\theta), \quad v_\theta(r, \theta) = -2a \sin(\theta) \quad (44)$$

Geometrically this flow field is comprised of a radial flow, scaled by the coefficient $b\cos(\theta)$, and a pure translation along the z -axis, scaled by the coefficient a .

Two boundary conditions are available for determining a , b , and c . The boundary conditions are, first, that the flow velocity at the point of contact with the projectile nose must equal the projectile nose velocity, and second, that the radial velocity component is zero at the outer edge of the flow field:

$$v_r(R, 0) = V, \quad v_r(\alpha R, 0) = 0 \quad (45)$$

The only material flow out of the region occurs through the $\theta = \pi/2$ surface. Assuming $c = 0$, these boundary conditions yield the velocity field:

$$v_r = \frac{V}{(\alpha^2 - 1)} \left(\frac{\alpha^2 R^2}{r^2} - 1 \right) \cos(\theta), \quad v_\theta = \frac{V}{\alpha^2 - 1} \sin(\theta) \quad (46)$$

This is the simplest velocity field for the hemispherical penetration problem. The velocity field has a shearing surface on the hemisphere boundary, where $v_\theta(\alpha R, \theta) \neq 0$. It is possible to remove this shearing surface by using the c term in the potential to force $v_\theta(\alpha R, \theta) = 0$. However, this subsequently gives rise to much more tedious calculations. In the following, the shearing surface will be ignored.

To calculate the plastic dissipation, the rigid plastic assumption will be made, since this velocity field is incompressible. The rate of deformation tensor components are

$$D_{rr} = \frac{\partial v_r}{\partial r} = -\frac{2V}{(\alpha^2 - 1)} \frac{\alpha^2 R^2}{r^3} \cos(\theta), \quad D_{\theta\theta} = \frac{v_\theta}{r} \cot(\theta) + \frac{v_r}{r} = \frac{V}{(\alpha^2 - 1)} \frac{\alpha^2 R^2}{r^3} \cos(\theta), \quad D_{r\theta} = 0, \quad (47)$$

$$D_{\theta\theta} = \frac{1}{r} \frac{\partial v_\theta}{\partial \theta} + \frac{v_r}{r} = \frac{V}{(\alpha^2 - 1)} \frac{\alpha^2 R^2}{r^3} \cos(\theta), \quad D_{r\theta} = \frac{1}{2} \left[\frac{1}{r} \frac{\partial v_r}{\partial \theta} + \frac{\partial v_\theta}{\partial r} - \frac{v_\theta}{r} \right] = -\frac{V}{2(\alpha^2 - 1)} \frac{\alpha^2 R^2}{r^3} \sin(\theta), \quad D_{\theta\theta} = 0$$

This gives a plastic strain rate

$$\dot{\epsilon}^p = \frac{V}{(\alpha^2 - 1)} \frac{\alpha^2 R^2}{r^3} \frac{1}{\sqrt{3}} \sqrt{12 - 11 \sin^2(\theta)} \quad (48)$$

which can be explicitly integrated to give the total dissipation rate \dot{W}_p :

$$\dot{W}_p = 2\pi Y_t \left\{ 1 + \frac{1}{\sqrt{132}} \ln(\sqrt{11} + \sqrt{12}) \right\} V R^2 \frac{\alpha^2 \ln(\alpha)}{\alpha^2 - 1} \quad (49)$$

The plastic dissipation is a monotonically increasing function of α .

Since the centerline momentum balance equation works well, the terms from it and from the energy-rate balance approach will be compared. The dissipation term from the rigid plastic energy rate balance, after division by $\pi R^2 V$, is

$$2Y_t \left\{ 1 + \frac{1}{\sqrt{132}} \ln(\sqrt{11} + \sqrt{12}) \right\} \frac{\alpha^2 \ln(\alpha)}{\alpha^2 - 1} = (2.333199...) \frac{\alpha^2 \ln(\alpha)}{\alpha^2 - 1} Y_t \quad (50)$$

and the shear stress term from the momentum balance (Eq. (39)) is

$$\frac{7}{3} \ln(\alpha) Y_t = (2.333333...) \ln(\alpha) Y_t \quad (51)$$

This identifies the plastic dissipation term in the energy-rate balance with the shear-stress term in the momentum balance. They are so similar because the momentum balance stress off the centerline was derived using rigid-plastic assumptions (see Walker and Anderson [1]).

As the projectile penetrates, it does work on the target. Within the target, the energy is partitioned into three modes: kinetic energy in the target, energy dissipated through plastic flow, and energy stored in elastic deformation. Equation (49) addresses energy dissipated through plastic flow. It is now necessary to include in the energy-rate balance the mechanisms of energy transfer into target kinetic energy and elastic compression energy. Based on the assumed hemispherical velocity field, it is possible to calculate the kinetic energy in the target in the vicinity of the front of the projectile:

$$E_k = \int_{\Omega} \frac{1}{2} \rho_t |\vec{v}|^2 d\Omega = \pi \rho_t \frac{V^2 R^3}{3(\alpha^2 - 1)^2} \{ \alpha^4 - 2\alpha^3 + 2\alpha^2 - 1 \} \quad (52)$$

As penetration occurs, some amount of energy is being continuously transferred into the target. While the target is doing work on the projectile, energy is being deposited in the target as kinetic and elastic energy. If the target is thought of as comprising stacked cylinders (as is often the case when cylindrical cavity expansion models are used to compute penetration), once the projectile passes through a cylinder of material the kinetic energy and elastic energy in the target will be transformed into another form - eventually dissipated through plastic flow - but while the projectile is doing work on the target, the energy is transferred into kinetic and elastic energy in the target and that mechanism determines the forces on the projectile. In order to estimate the rate at which energy is transferred into kinetic energy within the target using Eq. (52), it is necessary to obtain a length scale. In rough terms, the volume of target material in the hemispherical velocity field is $(2/3)\pi(\alpha R)^3$. To convert this to a cylinder, consider a cylinder of radius αR and height αh . Equating volumes gives $h = 2R/3$. Dividing E_k by h gives a work per unit distance that is being deposited in target kinetic energy:

$$\frac{E_k}{h} = \pi \rho_t \frac{u^2 R^2}{2(\alpha^2 - 1)^2} \{\alpha^4 - 2\alpha^3 + 2\alpha^2 - 1\} \approx (0.35 \text{ to } 0.40) \rho_t u^2 \pi R^2 \quad (53)$$

where the values are for α ranging from 2 to 10. Multiplication by u gives the work rate that goes into the kinetic energy in the target in an energy rate balance the term. To compare with the momentum balance, divide by $\pi R^2 u$ to obtain

$$\frac{\dot{W}_{KE}}{\pi R^2 u} = u \frac{E_k}{h} / (\pi R^2 u) = (0.35 \text{ to } 0.40) \rho_t u^2 \quad (54)$$

Thus, according to this reasoning, the energy transfer into target kinetic energy is the mechanism accounting for the majority of the $(1/2)\rho u^2$ term seen in the centerline momentum balance equation. Unfortunately, the assumption of an incompressible velocity field does not allow the calculation of energy in elastic compression.

Using the cavity expansion model to predict the mechanism of energy transfer allows calculation of both kinetic and elastic compressive energy terms. The energy loss rate of the projectile is set equal to

$$u \{(E_k)_{2D} + (E_e)_{2D} + (W_p)_{2D}\} = u \left\{ \frac{1}{2} \rho u^2 \pi R^2 (\dots) + \frac{1}{2} \rho u^2 \pi R^2 [\dots] + \pi R^2 Y \{\dots\} \right\} \quad (55)$$

The coefficients in the brackets are given in Eqs. (32), (33), and (38). When divided by $\pi R^2 u$ the target resistance from the energy rate balance from the cavity expansion is

$$\frac{1}{2} \rho u^2 (\dots) + \frac{1}{2} \rho u^2 [\dots] + Y \{\dots\} \quad (56)$$

Comparison with the momentum balance shows that the $(1/2)\rho u^2$ term originates from the transfer of energy to the target in the form of kinetic and elastic energy and the Y term is from plastic dissipation. To directly compare, Fig. 7 shows the values of the coefficients for the E_k , E_e and W_p terms; the first two would sum to 1 if the approaches were exactly the same, and the third would equal $7/3 \log(c_0/u) Y$, (shown in the plot). It can be seen that the coefficients are larger than expected for small velocities, and decrease with increasing velocity. The E_k and E_e coefficients sum to 1 for $\alpha = 1.6$. The material constants used in this plot are those previously stated for steel.

Since energy is being transferred to kinetic and elastic compressive energies at a rate that is a function of the penetration velocity squared, it is seen that the resisting force on the projectile also increases as a function of velocity squared. This explains why increasing impact velocities do not produce large increases in depths of penetration - though the energy that goes into initial plastic dissipation does not greatly increase, the energy that is transferred from the projectile into kinetic energy and elastic energy in the target does greatly increase. Though eventually nearly all the energy will be dissipated through plastic flow, it is the transfer mechanism at the time the projectile is penetrating that determines resistance.

For the energy-rate balance models to be similar to momentum balance models, it is necessary to include the mechanism of energy transfer within the target. Even though the global kinetic energy in the target is

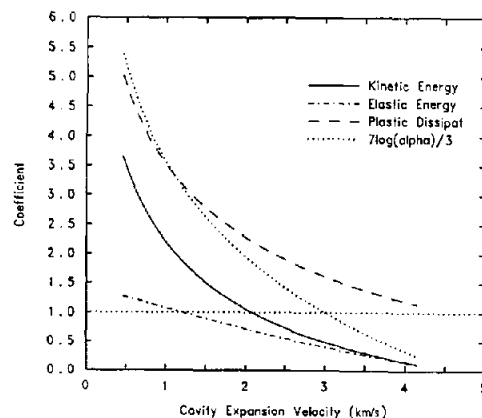


Fig. 7. Coefficients from cavity expansion.

relatively constant for high velocity eroding penetration, the mechanics of how the energy is being supplied to the target in kinetic and elastic forms is central to calculating the force that decelerates the projectile. The fact that the energy later plastically dissipates in the target is not enough information to determine the penetration and penetration history of the projectile.

To compare with the numerical results, it is necessary to have some idea of how the kinetic energy is later dissipated as plastic work in the target. Once the target is put in motion, it continues to move until the energy is dissipated. Based on the work above for penetration, an upper bound on the time is obtained by just balancing the change in kinetic energy against the work lost through plastic dissipation for the two-dimensional cavity expansion (Eqs. (32) and (38)). Letting

$$c_4(\bar{\xi}) = 2 \left\{ \frac{2}{\sqrt{1-\bar{\xi}^2}} \ln \left(\frac{\sqrt{1-\bar{\xi}^2}}{\bar{\xi}} + \frac{1}{\bar{\xi}} \right) - 1 \right\} \left(\frac{-2 \ln(\bar{\xi})}{1-\bar{\xi}^2} - 1 \right)^{-1} \quad (57)$$

contain all the terms that depend on $\bar{\xi}$, and assuming that $\bar{\xi}$ remains constant gives

$$\dot{E}_K + W_p = 0 \quad \Rightarrow \quad \rho R V^2 \dot{R} + \rho R^2 V \dot{V} + Y V R c_4(\bar{\xi}) = 0 \quad (58)$$

Equation (58) assumes that the cavity is no longer driven, and is only a very rough estimate of behavior since the actual problem is not being solved. What is of interest here is the form of the behavior and the time scale. Noting that $\dot{R} = V$, this can be integrated to give

$$R V = R_0 V_0 (1 - t/t_f) \quad \text{where } t_f \equiv \rho R_0 V_0 / Y c_4(\bar{\xi}) \quad (59)$$

In particular, this implies that the kinetic energy, which depends on $(R V)^2$ (see Eq. (32)), behaves as

$$E_K \sim (E_K)_0 (1 - t/t_f)^2 \quad (60)$$

This form can be used to get some idea of the kinetic energy behavior in the target. The following arguments assume an eroding penetration is occurring at a roughly constant penetration velocity u . During early penetration, energy is dumped into the target in the form of target kinetic energy faster than it is being dissipated away, and so the kinetic energy in the target is increasing. When a steady portion of penetration is reached, the amount of energy dumped into the target in kinetic energy equals the amount of the target's kinetic energy that is lost to dissipation. The steady portion of penetration lasts until the rod has completely eroded. After the rod has eroded, the kinetic energy in the target continues to be dissipated:

$$E_K \sim \int_0^t (E_K)_{2D} u \left(1 - \frac{t-\tau}{t_f} \right)^2 d\tau = (E_K)_{2D} \frac{u t_f}{3} \begin{cases} 1 - (1 - t/t_f)^3, & 0 \leq t < t_f \\ 1, & t_f \leq t < t_{\text{eroded}} \\ (1 - (t - t_{\text{eroded}})/t_f)^3, & t_{\text{eroded}} \leq t \leq t_{\text{eroded}} + t_f \end{cases} \quad (61)$$

Figure 8 shows qualitatively the expected time dependence. This curve qualitatively agrees with the target kinetic energies to be presented next.

Full scale hydrocode calculations were performed with CTH (McGlaun, *et al.* [10]), similar to those seen in Anderson, *et al.* [11]. The $L/D=10$, 10 cm long projectile was tungsten, modeled with a Mie-Grüneisen equation of state ($\rho=17.6 \text{ g/cm}^3$, $c_0=3.85 \text{ km/s}$, $s=1.44$, $\gamma_0=1.48$) and an elastic-perfectly plastic constitutive model with a flow stress of 1.5 GPa and $\nu=0.30$, and the target was steel, modeled with a Mie-Grüneisen equation of state ($\rho=7.85 \text{ g/cm}^3$, $c_0=4.5 \text{ km/s}$, $s=1.49$, $\gamma_0=2.17$) and an elastic-perfectly plastic constitutive model with a flow stress of 1.2 GPa and $\nu=0.29$. The various components to the energy are shown in Figs. 9–11 for impact velocities of 1.5 km/s, 3.0 km/s and 4.5 km/s. The projectile kinetic energy is seen to decrease, mostly through erosion. The total target energy is seen to increase in almost like fashion. (It is noticeably less for the 1.5 km/s impact, where the amount of energy lost to plastic deformation of the projectile is about 11%. The total energy dissipated internally within the projectile is nearly independent of impact velocities — about 20 KJ for this projectile-

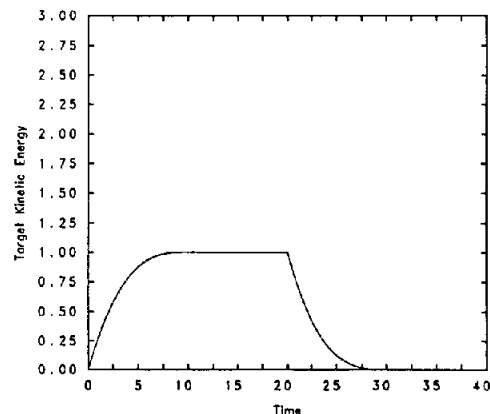


Fig. 8. Behavior of kinetic energy in target expansion.

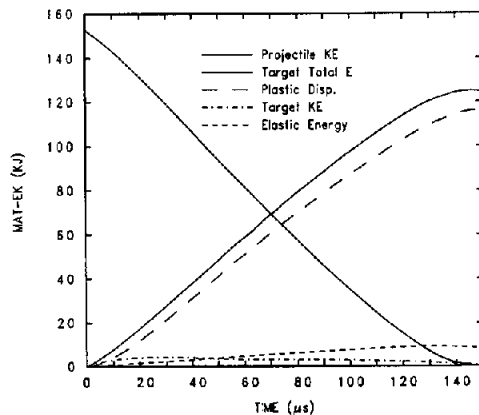


Fig. 9. Energy for 1.5 km/s tungsten into steel.

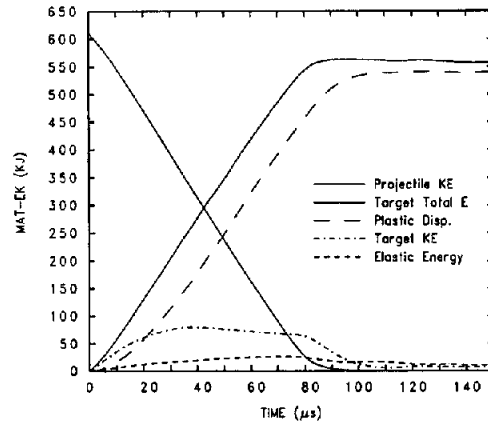


Fig. 10. Energy for 3.0 km/s tungsten into steel.

so as the impact velocity goes up the relative percentage goes down. Equating this energy rise to plastic work gives an average strain in the eroded projectile material of 170%.) Large amounts of kinetic energy in the target are seen at the higher impact velocities (the 4.5 km/s case is still rising when the projectile completely erodes at about 55 μ s), but even for the 1.5 km/s impact velocity the amount is relevant, even though small. Given the interpretation of energy transfer mechanisms given above, the relative rate of energy initially going into target kinetic energy and elastic compression energy can be obtained through the ratio $(1/2)\rho u^2 / \{(1/2)\rho u^2 + (7/3)\ln(c_0/u)Y_t\}$. For the three impact velocities here, the CTH computations give penetration velocities of approximately 700 m/s, 1700 m/s, and 2650 m/s, which give the amount of energy being transferred into kinetic and elastic energy at 27%, 81% and 95% of the total energy transfer for the 1.5 km/s, 3.0 km/s, and 4.5 km/s impacts, respectively. Thus, for higher velocities, initially most of the energy is delivered into the target through these mechanisms, highlighting the actual energy transfer mechanism's importance.

With the computations the time it takes the kinetic energy and elastic energy in the target to dissipate (though these may be different) can be estimated. The rate of energy transfer to the target for each of the cases is roughly 1.18 KJ/ μ s, 7.2 KJ/ μ s, and 25 KJ/ μ s, and the "steady state" value of the energy stored in the target in kinetic and elastic energy is estimated to be 8.6 KJ, 95 KJ, and 560 KJ, for the three respective velocities. Using Eq. (61), the time it takes for the energy to dissipate is given by 3 times the steady state energy divided by the energy transfer rate. These values give dissipation times of 22 μ s, 40 μ s, and 67 μ s for the 1.5, 3.0, and 4.5 km/s impacts, respectively. These dissipation times roughly scale with velocity, and are short enough to show why even though most of the energy is being initially deposited in the target in kinetic and elastic energy, large amounts of accumulated energy in these forms are not seen.

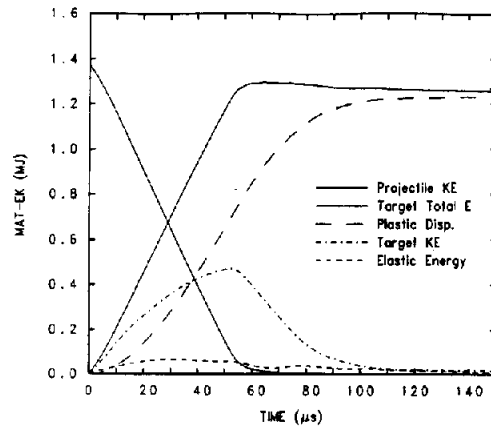


Fig. 11. Energy for 4.5 km/s tungsten into steel.

CONCLUSIONS

The mechanisms of energy transfer into a target during impact have been detailed. The projectile energy is initially transformed into target kinetic energy, elastic compression energy and plastic dissipation. As impact velocity increases, more and more energy during the penetration event is temporarily deposited within the target as elastic compression and target kinetic energy. This energy will be dissipated by the target at a later time, but at the time of penetration these energy transfer mechanisms define the force acting on the projectile. Thus, for an energy-rate balance approach to successfully model penetration, it must include the transfer of energy into kinetic energy within the target and the storage of energy by elastic compression. Understanding the role of energy dissipation in the target clarified the various terms in analytic models and identified their origin in terms of the fundamental physics. Thus, even though the

initial kinetic energy of the projectile is increasing as the impact velocity squared, the energy transfer rate to the target increases in the same fashion, and thus there is only a slow increase in penetration depth with increasing velocity.

Acknowledgements—The author appreciates the help and discussion with Chris Freitas, Charles E. Anderson, Jr., and Dick Sharron, all of Southwest Research Institute.

REFERENCES

- [1] Walker JD, Anderson Jr. CE. A Time-Dependent Model for Long-Rod Penetration. *Int. J. Impact Engng.* 1995; 15(2): 19–48.
- [2] Hinze JO. *Turbulence*, MacGraw-Hill, New York, 1975.
- [3] Hill R. *The Mathematical Theory of Plasticity*, Oxford University Press, Oxford, 1950.
- [4] Lubliner J. *Plasticity Theory*, Macmillan Publishing Co., New York, 1990.
- [5] Malvern LE. *Introduction to the Mechanics of a Continuous Medium*, Prentice-Hall, Englewood Cliffs, NJ, 1969.
- [6] Walker JD. On Maximum Dissipation for Dynamic Plastic Flow. Final Report, SwRI Project No. 07-9753, San Antonio, TX, 1995.
- [7] Crozier RJM, Hunter SC. Similarity Solution for the Rapid Uniform Expansion of a Cylindrical Cavity in a Compressible Elastic-Plastic Solid. *Quart. Journ. Mech. and Applied Math.* 1970; 23(3): 349–363.
- [8] Forrestal MJ, Brar NS, Luk VK. Penetration of Strain-Hardening Targets with Rigid Spherical-Nose Rods. *J. Appl. Mech.* 1991; 58: 7–10.
- [9] Forrestal MJ, Luk VK. Dynamic Spherical Cavity-Expansion in a Compressible Elastic-Plastic Solid. *J. Appl. Mech.* 1988; 55: 275–279.
- [10] McGlaun JM, Thompson SL, Elrick MG. CTH: A Three-Dimensional Shock Wave Physics Code. *Int. J. Impact Engng.* 1990; 10: 351–360.
- [11] Anderson Jr. CE, Littlefield DL, Walker JD. Long-Rod Penetration, Target Resistance, and Hypervelocity Impact. *Int. J. Impact Engng.* 1993; 14: 1–12.
- [12] Tate, A. A Theory for the Deceleration of Long Rods After Impact, *J. Mech. Phys. Solids.* 1967; 15: 387–399.
- [13] Alekseevskii, VP. Penetration of a Rod into a Target at High Velocity. *Combustion, Explosion and Shock Waves.* 1966; 2: 63–66.

APPENDIX: ENERGY-RATE BALANCE TO TATE

This appendix demonstrates how energy-rate balance arguments can give rise to the simplified penetration model of Tate [12] and Alekseevskii [13]. The connection for the momentum balance is simple and direct (as shown in Walker and Anderson [1]), and can be seen from Eq. (39) in the main text by taking the limit as the three-dimensional model terms are allowed to go to zero: $s \rightarrow 0$ and $R \rightarrow 0$ gives

$$-\rho_p \dot{v}L + \frac{1}{2}\rho_p(v-u)^2 = \frac{1}{2}\rho_p u^2 + \frac{7}{3}\ln(\alpha)Y_p, \quad \dot{v} = -\frac{\sigma_p}{\rho_p L} \quad (A1)$$

The identification of σ_p with Y_p and $(7/3)\ln(\alpha)Y_p$ with R , gives the model of Tate.

In order to similarly obtain the Tate and Alekseevskii formulation with energy-rate arguments is either extremely difficult or requires a number of significant assumptions, as might be guessed due to the conclusions of the main text of this paper. To pursue a simple derivation, it will be assumed that the energy deposition in the target can be partitioned into two parts: a forward work part that represents the energy required to increase the depth of the crater, and a lateral work part that represents the energy required to open up the crater. In a similar fashion, the change in kinetic energy of the projectile will be partitioned into a loss of kinetic energy in the forward direction and a loss in the lateral direction. The work required to increase the depth of the crater will then be equated to the energy loss in the forward direction for the projectile. In reality, such a partitioning is questionable since energy is a scalar quantity and there is doubt that it is possible to separate the work required to increase the depth of a crater from the work required to open up the crater in the first place. However, as the paper has argued, to arrive at the simple formulation of Tate and Alekseevskii with an energy model requires a complete model that includes energy transfer mechanisms, and the partitioning proposed here is an attempt to reflect the effects of some of those mechanisms.

First consider the kinetic energy of the projectile. The projectile rear velocity is v and the projectile penetration velocity is u . Assuming minimal internal energy loss within the projectile due to projectile erosion, projectile material is deflected to move in the perpendicular direction at a velocity $v-u$. Thus, when eroded projectile material leaves the projectile it has a kinetic energy based on the velocity $\tilde{v} = \sqrt{u^2 + (v-u)^2}$. The kinetic energy of projectile material is thus

$$E_p = A_p \left\{ \frac{1}{2}\rho_p v^2 L + \int_L^{L_0} \frac{1}{2}\rho_p \tilde{v}^2(L) dL \right\} \quad (A2)$$

where A_p is the cross sectional area of the projectile and the integral represents the kinetic energy in the eroded projectile material at the time of erosion (\tilde{v} is viewed as a function of residual projectile length). Differentiation with respect to time gives

$$\dot{E}_p = A_p \left\{ \rho_p v \dot{L} + \frac{1}{2} \rho_p v^2 \dot{L} - \frac{1}{2} \rho_p \tilde{v}^2(L) \dot{L} \right\} = A_p \{ \rho_p v \dot{L} - \rho_p (v - u)^2 u \} \quad (A3)$$

For the target, the work rate assumed for increasing the depth of penetration is approximated by

$$\dot{W}_t = -A_c \left(\frac{1}{2} \rho_t u^2 + \frac{7}{3} \ln(\alpha) Y_t \right) u \quad (A4)$$

where A_c is the area at the front of the crater being worked on. Equating \dot{E}_p and \dot{W}_t requires that the ratio A_p/A_c be determined. To estimate the ratio, if the projectile density change is assumed minimal (which it is) and if the radial velocity of the projectile material were minimal (which it is not), then it is possible to show that mass conservation implies $\partial(Av)/\partial x = 0$ and therefore it will be assumed that $A_p/A_c = u/v$. With this assumption, equating the projectile energy rate with the target work rate gives

$$-\rho_p v \dot{L} + \frac{u}{v} \rho_p (v - u)^2 = \frac{1}{2} \rho_t u^2 + \frac{7}{3} \ln(\alpha) Y_t \quad (A5)$$

which recovers the form of Tate and Alekseevskii since it is often the case that $u/v \sim 1/2$.